

The Highest Redshift Quasars: Early Black Hole Growth and the End of Reionization Epoch

Xiaohui Fan

Steward Observatory, The University of Arizona, 933 North Cherry Avenue, Tucson, AZ 85721-0065, USA

Abstract. The discovery of luminous quasars at $z > 6$ indicates the existence billion-solar-mass black holes at the end of reionization epoch. directly probing the early growth of supermassive black holes in the universe and the relation between the formation of early galaxies and black holes. Absorption spectra of these quasars trace the evolution of intergalactic medium (IGM). Currently, more than 25 quasars have been discovered at $z > 5.5$, including 13 at $z > 6$. In this proceeding, I review the recent observational results studies of the highest redshift quasars, including the evolution of quasar density and luminosity function, the evolution of their spectral properties and chemical enrichment history. I will also discuss using quasar spectra to probe the evolution of ionization state of the end of reionization epoch.

1. Introduction

Discoveries of luminous quasars at $z > 6$ shows that active, massive black holes of the order billion solar masses existed a few hundred million years after the first star formation in the Universe (Spergel et al. 2007), at the end of the reionization epoch. How does the black hole population grow with cosmic time? How does the evolution of quasar density traces the accretion history of early supermassive black holes? Locally, the tight correlation between the mass of central BHs and the velocity dispersion of host galaxies implies that black hole activities and galaxy formation are strongly coupled. How are the formation of galaxies and black hole activities related at early epochs? Finally, the detection of complete Gunn-Peterson (Gunn & Peterson 1965) troughs in the highest redshift quasars (Becker et al. 2001; Djorgovski et al. 2001; Fan et al. 2002; White et al. 2003) marks the reionization process ended at $z \sim 6$. What is the role of black hole accretion power played in the reionization of the Universe? Detailed observations of the highest-redshift quasars known provide crucial answers to these important questions about quasar formation, galaxy evolution and the evolution of intergalactic medium (IGM).

2. Evolution of Quasar Density and Luminosity Function at High-Redshift

Quasars with redshift greater than 5.7 are characterized by very red $i - z$ colors. Since 2000, we have been using the imaging data from the SDSS to select i -dropout candidates. At $z > 5.7$, all quasars have deep Ly α absorption and satisfy our color-selection criteria ($i - z > 2.2$). In a series of papers (Fan et al.

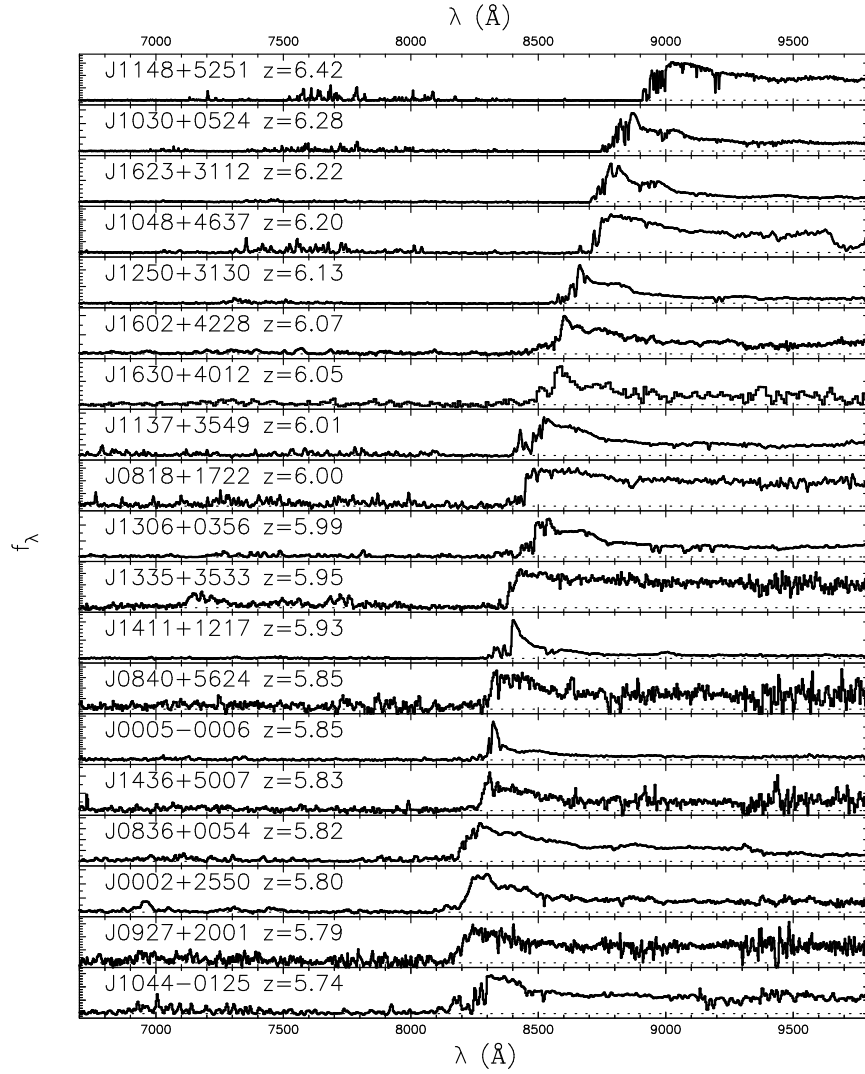


Figure 1. Low-dispersion spectra of the nineteen published SDSS quasars (Fan et al. 2006b) at $z > 5.7$. Note the strong Ly α absorption blueward of Ly α emission and the existence of strong metal emission lines in the spectra.

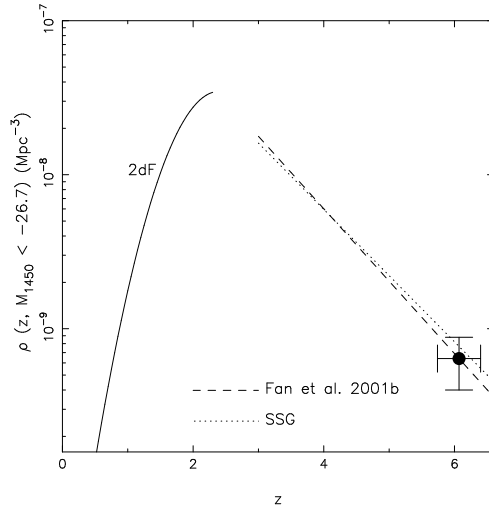


Figure 2. The evolution of the quasar comoving spatial density at $M_{1450} < -26.7$. The filled circle represents the result from this survey. The error-bar in redshift indicates the redshift range covered by the *i*-dropout survey. The dashed and dotted lines are the best-fit models from Fan et al. (2001) and Schmidt, Schneider, & Gunn (1995), respectively. The solid line is the best-fit model from the 2dF survey (Croom et al. 2004) at $z < 2.3$. Adapted from Fan et al. (2004).

2001, 2003, 2004, 2006a), we reported the selection and identification of nineteen quasars selected from about 6600 deg^2 of SDSS imaging. The sample covers the redshift range $z = 5.74 - 6.42$, and a range of absolute magnitudes in rest-frame 1450\AA , $M_{1450} = -26.2$ to -27.9 . Figure 1 shows the spectra of the nineteen SDSS quasars at $z > 5.7$.

The density of luminous quasars is a strong function of redshift: it peaks at $z \sim 2 - 3$ and declines exponentially towards lower and higher redshift (e.g. Schmidt, Schneider, & Gunn 1995; Boyle et. al. 2000). Compared to the evolution of star-formation rate in the Universe, the quasar density peaks at higher redshift, and evolves much faster. This exponential decline continues to the highest redshifts. In Figure 2, we present the density of quasars at $M_{1450} < -26.7$ found in 6000 deg^2 of SDSS data at $z \sim 6$, along with the results from lower redshift (Schmidt, Schneider, & Gunn 1995; Boyle et. al. 2000; Fan et al. 2001). The quasar density at $z \sim 6$ found here is consistent with extrapolating the best-fit quasar luminosity functions in the range $3 < z < 5$. The comoving density of luminous quasars at $z \sim 6$ is ~ 40 times smaller than that at $z \sim 3$, as we close in to the epoch of the formation of first supermassive black holes in the Universe.

The existence of these objects is amazing feat of galaxy formation process. The SDSS $z \sim 6$ quasars are among the most luminous quasars at any redshift; their apparent magnitudes are ~ 19 even at $z > 6$! They are likely powered by supermassive black holes with several billion solar masses, and reside in dark matter halo of $10^{13} M_{\odot}$. They are among the most massive black holes and

galaxies at any redshifts. It is a challenge as how the universe could have formed with such massive galaxies, and in particular, have assembled such massive black holes in the first Gyr of the cosmic evolution. They are clearly the rarest and most biased systems in the early universe, and probably have started the initial assemble at redshift much higher than 10, well into the dark ages, providing important clues to the co-formation and co-evolution of the earliest supermassive black holes and galaxies.

3. Spectral Evolution and Black Hole Mass at High-Redshift

The spectral energy distributions of luminous quasars show little evolution out to high redshift. There is growing evidence from emission line ratio measurements that quasar broad emission line regions have roughly solar or even higher metallicities at $z > 4$ (e.g. Hamann & Ferland 1993), similar to that in low redshift quasars. Dietrich et al. (2003) found the FeII/MgII ratio to have roughly the same value in a sample of $z \sim 5$ quasars as at lower redshift, suggesting that the metallicity of quasar emission line region remains high to even earlier epochs. Optical and infrared spectroscopy of some $z \sim 6$ quasars already indicates *a lack of evolution* in the spectral properties of these luminous quasars: Pentericci et al. (2002) show that the CIV/NV ratio in two $z \sim 6$ quasars are indicative of supersolar metallicity in these systems. Freudling, Corbin, & Korista (2003) and Barth et al. (2003) detected strong FeII emission in the spectra of four $z \sim 6$ SDSS quasars. In addition, the optical-to-X-ray flux ratios and X-ray continuum shapes show at most mild evolution from low redshift (e.g. Vignali et al. 2003). Figure 3 shows the composite of our $z \sim 6$ quasar spectra: it is almost identical to the low- z composite, both in term of the spectral slope, and emission line strength.

The black hole mass estimates of the $z \sim 6$ SDSS quasars ranging from several times $10^8 M_\odot$ to several times $10^9 M_\odot$. Assuming continuous Eddington accretion from a seed black hole of $100 M_\odot$, the formation redshift for seed black holes must be at $z > 10$. Even with continuous accretion, black holes in the most luminous quasars barely had enough time growing. While there are various ways of accreting faster than Eddington, the fact that the highest redshift quasars sit right at the threshold of the reionization epoch simply indicate that the initial growth of those BHs have to be very efficient and very early on.

The lack of spectral evolution in high-redshift quasars is not limited to the rest-frame UV, it is also evident in X-ray and near to mid-IR. Strateva et al. (2005) studied the evolution of α_{OX} , the power law index between soft X-ray and optical, for a large sample of quasars at $z = 0 - 6$. They found that when taken into account the dependence of α_{OX} on UV luminosity, there is no any evidence of evolution in the X-ray emission of quasars. However, there finally appear to be sign of evolution in the infrared wavelengths: we have carried out Spitzer observations of thirteen $z \sim 6$ quasars using the IRAC and MIPS instruments (Jiang 2006). We find that most of these quasars have prominent emission from hot dust as evidenced by the observed 24um fluxes. Their spectral energy distributions (SEDs) are similar to those of low-redshift quasars at rest-frame 0.15-3.5 μm , suggesting that accretion disks and hot-dust structures for these sources already have reached maturity. However, one of the $z \sim 6$ quasar,

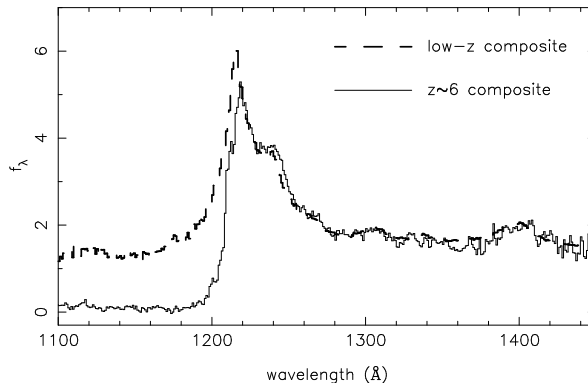


Figure 3. The composite spectrum of $z \sim 6$ quasars (solid line). For comparison, we also plot the low-redshift quasar spectral composite from Vanden Berk et al. (2001). The effective redshift in the 1000 – 1500Å range in the Vanden Berk et al. composite is about 2. The quasar intrinsic spectrum redward of Ly α emission shows no detectable evolution up to $z \sim 6$, in terms of both the continuum shape and emission line strengths. On the blue side of Ly α emission, the strong IGM absorption at $z \sim 6$ removes most of the quasar flux. Adapted from Fan et al. (2004).

SDSS J0005-0006 has an unusual SED that lies significantly below low-redshift SED templates at rest-frame 1 and 3.5 μm , and thus shows a strong near-IR (NIR) deficit and no hot-dust emission. Type I quasars with extremely small NIR-to-optical flux ratios like SDSS J0005-0006 are not found in low-redshift quasar samples, indicating that SDSS J0005-0006 has different dust properties at high redshift.

4. Evolution of IGM Ionization State

We study the evolution of the ionization state of the intergalactic medium (IGM) at the end of the reionization epoch using moderate resolution spectra of SDSS quasars at $z > 5.5$. Three methods are used to trace IGM properties: (a) the evolution of the Gunn-Peterson (GP) optical depth in the Ly α , β , and γ transitions; (b) the distribution of lengths of dark absorption gaps, and (c) the size of HII regions around luminous quasars.

Using this large sample, we find that the evolution of the ionization state of the IGM accelerated at $z > 5.7$ (Figure 4): the GP optical depth evolution changes from $\tau_{\text{GP}}^{\text{eff}} \sim (1+z)^{4.3}$ to $(1+z)^{>11}$, and the average length of dark gaps with $\tau > 3.5$ increases from < 10 to > 80 comoving Mpc. The dispersion of IGM properties along different lines of sight also increases rapidly, implying fluctuations by a factor of > 4 in the UV background at $z > 6$, when the mean free path of UV photons is comparable to the correlation length of the star forming galaxies that are thought to have caused reionization. The mean length of dark gaps shows the most dramatic increase at $z \sim 6$, as well as the largest line-of-sight variations. We suggest using dark gap statistics (Songaila &

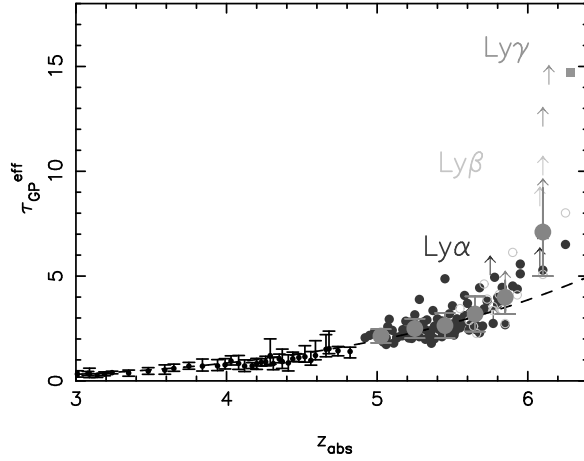


Figure 4. Evolution of optical depth with combined the Ly α , Ly β and Ly γ results. The Ly β measurements are converted to Ly α GP optical depth using a conversion factor of 2.25. The values in the two highest redshift bins are lower limits since they both contain complete GP troughs. The dashed line is a redshift evolution of $\tau_{\text{GP}}^{\text{eff}} \propto (1+z)^{4.3}$. At $z > 5.5$, the best fit evolution has $\tau_{\text{GP}}^{\text{eff}} \propto (1+z)^{10.9}$, indicating an accelerated evolution. The large filled symbols with error bars are the average and standard deviation of optical depth at each redshift. The sample variance also increases rapidly with redshift.

Cowie 2002) as a powerful probe of the ionization state of the IGM at yet higher redshift. Some dark gaps as long as 50 comoving Mpc appear by $z \sim 5.7$, while other line of sight at $z > 6$ is still somewhat transparent.

UV photons from a luminous quasar will ionize a HII region (Madau & Rees 2000; Cen & Haiman 2000) in the IGM. In the early Universe, the quasar HII region size scales as $R_s \propto (\dot{N}_Q/2f_{\text{HI}})^{1/3}$, where \dot{N}_Q is the number of ionizing photons the central quasar emits per unit time, and f_{HI} is the IGM neutral fraction. We have measured sizes of proximity zone around luminous SDSS quasars (Fan et al. 2006b) and found that they decrease rapidly towards higher redshift, by a factor of ~ 2.5 from $z = 5.7$ to 6.4 (Figure 5), suggesting that the neutral fraction of the IGM has increased by a factor of > 10 cover this narrow redshift range. This estimate is consistent with the value derived from the GP optical depth.

Based on the GP optical depth and HII region size measurements, we find that the mass-averaged neutral fraction is $1 - 4\%$ at $z \sim 6.2$. Moreover, the current observations are inconsistent with a mostly neutral IGM at $z \sim 6$, as indicated by the finite length of Gunn-Peterson troughs. Combining different measurements, we conclude that the IGM evolution is accelerated at $z \sim 6$, with an order of magnitude change in the ionization state and increased line of sight variations over a narrow redshift range. The observations suggest that $z \sim 6$ is the end of the overlapping stage of reionization, and are inconsistent with a mostly neutral IGM at $z \sim 6$, as indicated by the finite length of dark absorption gaps.

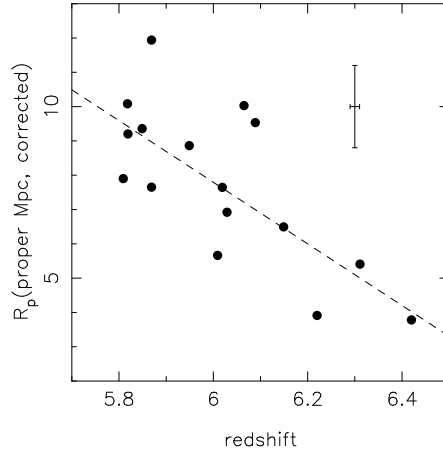


Figure 5. Size of quasar proximity zone as a function of the redshift of the quasar. The size R_p is the line of sight distance from the quasar to the point at which the transmitted flux ratio falls to 0.1 of the continuum level. The radius also has been scaled to a common absolute magnitude ($M_{1450} = -27$). The linear fit shows a factor of 2.8 decrease in the HII region size around quasars from $z = 5.7$ to 6.4. The error on R_p is dominated by the uncertainty in the quasar redshift.

Figure 6 shows the current limits on the cosmic neutral fraction versus redshift. The observations paint an interesting picture. On the one hand, studies of GP optical depths and variations, and the GP ‘gap’ distribution, as well as of the thermal state of the IGM at high z , and of quasar HII regions and surfaces around the highest redshift QSOs, suggest a qualitative change in the state of the IGM at $z \sim 6$. These data indicate a significant neutral fraction, $x_{HI} > 10^{-3}$, and perhaps as high as 0.1, at $z \geq 6$, as compared to $x_{HI} \leq 10^{-4}$ at $z < 5.5$. The IGM characteristics at this epoch are consistent with the end of the ‘percolation’ stage of reionization. On the other hand, transmission spikes in the GP trough and study of the evolution of Ly α galaxy luminosity function indicate a neutral fraction smaller than 50% at $z \sim 6.5$. Moreover, the measurement of the large scale polarization of the CMB suggests a significant ionization fraction extending to higher redshifts, $z \sim 11 \pm 3$. Combining these redshifts, it seems that current observation is right at the threshold of the peak of reionization era. It would be highly exciting to see what happens at $z = 7 - 8$, in particular whether the IGM has become mostly neutral by that point, resembling a phase transition, as has been hinted by Gunn-Peterson measurements, or that the reionization process had been a much gradual process that lasted for more than a couple of hundred million years.

References

- Barth, A. J., Martini, P., Nelson, C. H., & Ho, L. C. 2003, ApJ, 594, L95
 Becker, R. H. et al. 2001, AJ, 122, 2850

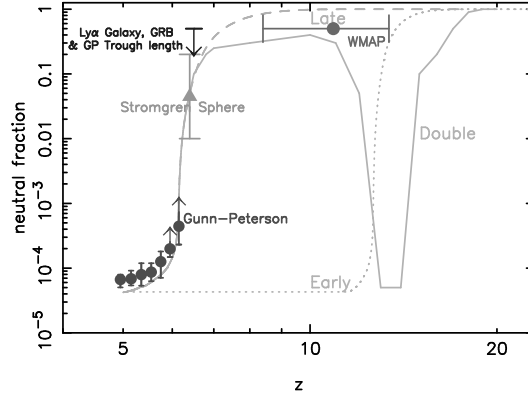


Figure 6. The volume averaged neutral fraction of the IGM versus redshift using various techniques. The dash line shows the fiducial model of Gnedin (2000) with late reionization at $z = 6 - 7$, the solid line shows an idealized model with double reionization as described in Cen (2003), and the dotted line illustrates the model with early reionization at $z \sim 14$.

- Boyle, B. J., Shanks, T., Croom, S. M., Smith, R. J., Miller, L., Loaring, B., & Heymans, C. 2000, MNRAS, 317, 1014
- Cen, R., & Haiman, Z. 2000, ApJ, 542, L75
- Cen, R. 2003, ApJ, 591, 12
- Croom, S. M., Smith, R. J., Boyle, B. J., Shanks, T., Miller, L., Outram, P. J., & Loaring, N. S. 2004, MNRAS, 349, 1397
- Dietrich, M., Hamann, F., Shields, J. C., Constantin, A., Heidt, J., Jaeger, M., Vestergaard, M., & Wagner, S. J. 2003, ApJ, 722, 732
- Djorgovski, S. G., Castro, S., Stern, D., & Mahabal, A. A. 2001, ApJ, 560, L5
- Fan, X. et al. 2001, AJ, 121, 54
- Fan, X. et al. 2002, AJ, 121, 123, 1247
- Fan, X. et al. 2003, AJ, 121, 125, 1649
- Fan, X. et al. 2004, AJ, 121, 128, 515
- Fan, X. et al. 2006a, AJ, 131, 1203
- Fan, X. et al. 2006b, AJ, 132, 117
- Freudling, W., Corbin, M. R., & Korista, K. T. 2003, ApJ, 587, L67
- Gnedin, N. 2000, ApJ, 535, 530
- Gunn, J. E., & Peterson, B. A. 1965, ApJ, 142, 1633
- Hamann, F., & Ferland, G. 1993, ApJ, 418, 11
- Jiang, L. 2006, AJ, 132, 2127
- Madau, P., & Rees, M. J. 2000, ApJ, 542, L69
- Pentericci, L. et al. 2002, AJ, 123, 2151
- Songaila, A., & Cowie, L. L. 2002, AJ, 123, 2183
- Schmidt, M., Schneider, D. P., & Gunn, J. E. 1995, AJ, 110, 68
- Spergel, D., Bean, R., O'Dore, M. et al. ApJS, 170, 377
- Strateva, I.V. et al. 2005, AJ, 130, 387
- Vignali, C., Brandt, W. N., Schneider, D. P., Garmire, G. P., & Kaspi, S. 2003, ApJ, 125, 2876
- White, R. L., Becker, R. H., Fan, X., & Strauss, M. A. 2003, AJ, 126, 1
- Vanden Berk, D. E. et al. 2001, AJ, 122, 549